

THS



This is to certify that the

thesis entitled

The Development of an Improved Quantitative Calibration for an Exciplex Liquid/Vapor Visualization System

presented by

Roy Stanley Schafer

has been accepted towards fulfillment of the requirements for

Master of Science degree in Mechanical Engineering

Heurld J. Schoole

Major professor

Date August 11, 1993

LIBRARY Michigan State University

PLACE IN RETURN BOX to remove this checkout from your record. TO AVOID FINES return on or before date due.

DATE DUE	DATE DUE	DATE DUE

MSU is An Affirmative Action/Equal Opportunity Institution cycle/classedus.pm3-p.1

THE DEVELOPMENT OF AN IMPROVED QUANTITATIVE CALIBRATION FOR AN EXCIPLEX LIQUID/VAPOR FUEL VISUALIZATION SYSTEM

By

Roy Stanley Schafer

A THESIS

Submitted to
Michigan State University
in partial fulfillment of the requirements
for the degree of

MASTER OF SCIENCE

Department of Mechanical Engineering

1993

ABSTRACT

THE DEVELOPMENT OF AN IMPROVED QUANTITATIVE CALIBRATION FOR AN EXCIPLEX LIQUID/VAPOR FUEL VISUALIZATION SYSTEM

By

Roy Stanley Schafer

Laser-induced fluorescence methods have recently been used for doing fuel distribution studies in internal combustion engines. Exciplex liquid/vapor visualization systems cause the liquid and vapor phases to fluoresce at different wavelengths when excited with an ultraviolet laser, thereby allowing two-dimensional fluorescent images of the two phases to be taken separately through bandpass filters.

Although the exciplex technique is not new, an improved quantitative calibration method has been developed relating fluorescence intensity to mass concentration of liquid and vapor fuel. An exciplex system composed of 1% N,N,N',N',-tetramethyl-p-phenylenediamine (TMPD), 10% naphthalene, and 89% n-decane by weight was used. The naphthalene/TMPD system is coevaporative with decane-based fuels such as diesel fuel. Such a calibration can then be used to do quantitative liquid and vapor fuel distribution studies.

ACKNOWLEDGMENTS

I would like to thank several people:

Dr. Harold Schock, my advisor, for his support which made it possible for me to go to graduate school, and the opportunity to be associated with the MSU Engine Research Laboratory.

Dr. Stanley Crouch for being on my advisory committee, for his assistance in helping me understand the photochemistry involved in this project, and for the use of his Isolated Droplet Generator which proved to be a reliable and stable instrument.

Dr. Craig Somerton for being on my advisory committee, for his guidance, and for the use of his temperature controllers.

Tom Stuecken for his assistance in the design and construction of the setup, and for teaching me how to "hog" some metal.

Dan McCarrick and Dr. Keunchul Lee for listening when I wanted to run ideas by them, and for giving their input.

Dr. John Funkhouser for his assistance, and for use of the Chemistry Department facilities for sample preparation.

The Glass Blowing shop in the Chemistry Department for assistance during sample preparation.

Ron Haas for loaning me the halogen leak detector during the repair of the excimer laser.

My parents, Stanley and Rose, and family for understanding why I missed so many family occasions.

I would also like to thank the NASA Lewis Research Center, Cleveland, Ohio and the Environmental Protection Agency, Ann Arbor, Michigan for supporting this work.

TABLE OF CONTENTS

LIST OF TAB	LES	page vi
LIST OF FIGU	JRES	Vii
CHAPTER 1 -	INTRODUCTION	1
	1.1 Introduction to Exciplex	1
	1.2 An Example of Fluorescent Images of a Fuel Distribution	3
CHAPTER 2 -	THE EXCIPLEX MECHANISM	6
	2.1 System Composition	6
	2.2 Separation of Phases	6
	EXPERIMENTAL EQUIPMENT AND CALIBRATION PROCEDURE	9
	3.1 Major Equipment	9
	3.1.1 UV - Visible Spectrophotometer	9
	3.1.2 Temperature-Controlled Sample Heating System	9
	3.1.3 Excimer Laser and Energy Meter	11
	3.1.4 Intensified CCD Detector	12
	3.1.5 Isolated Droplet Generator	13
	3.2 Procedure	15
	3.2.1 Vapor Phase	15

	3.2.1.	1 Sample Preparation		16
	3.2.1.		por Concentration Vers	
	3.2.1.		orescence Intensity Ver	
	3.2.2 Liquid	Phase		23
CHAPTER 4	- RESULTS AND DI	SCUSSION		27
	4.1 Vapor Phase			27
	4.2 Liquid Phase			31
CHAPTER 5	- SUMMARY AND	CONCLUSIONS		35
CHAPTER 6	- RECOMMENDAT	IONS		37
LIST OF REI	FERENCES			39
APPENDIX				41
		nections for Laser Indu	ced Fluorescence	41
	A.2 Operational Info	ormation for the Laser I	nduced Fluorescence	43

LIST OF TABLES

TABLE 1: Spectrophotometer settings used for making absorbance measurements.	page 18
TABLE 2: System components and parameter values for vapor phase calibration	. 20
TABLE 3: Average intensity gain versus potentiometer setting.	. 43
TABLE 4: Gate pulse width versus potentiometer setting.	. 44

LIST OF FIGURES

	page
FIGURE 1: Schematic of engine in which fluorescent images were taken	3
FIGURE 2: Fluorescent images of the fuel distribution in an engine cylinder	4
FIGURE 3: The mechanism of Exciplex liquid/vapor visualization systems	7
FIGURE 4: Fluorescence emission spectra of the liquid and vapor phases. (3)	8
FIGURE 5: Schematic of temperature-controlled sample heating system.	10
FIGURE 6: Schematic of the droplet formation module of the isolated droplet generator.	14
FIGURE 7: Schematic of setup for determining vapor concentration.	17
FIGURE 8: Schematic of setup for determining fluorescence intensity of vapor phase	. 19
FIGURE 9: Setup for determining vapor concentration.	21
FIGURE 10: Temperature-controlled sample heating system with insulation removed	. 22
FIGURE 11: Setup for determining fluorescence intensity of vapor phase	22
FIGURE 12: Schematic of setup for determining fluorescence intensity of liquid phase.	23
FIGURE 13: Setup for determining fluorescence intensity of liquid phase	25
FIGURE 14: Droplet formation module of the isolated droplet generator	25
FIGURE 15: Fluorescent image of isolated droplets.	26
FIGURE 16: A zoom of some individual droplets from Figure 15.	26
FIGURE 17: TMPD vapor concentration versus temperature for first step of vapor phase calibration	28

FIGURE 18: Normalized fluorescence intensity versus TMPD vapor concentration.	30
FIGURE 19: Normalized fluorescence intensity versus droplet mass.	32
FIGURE 20: Normalized fluorescence intensity versus liquid mass using multiple droplet summation.	34
FIGURE 21: Connections for laser induced fluorescence equipment.	41
FIGURE 22: Timing diagram for ICCD detector system configuration.	42

CHAPTER 1

INTRODUCTION

Controlling the fuel distribution in the combustion chambers of internal combustion engines is important for decreasing exhaust emissions and increasing efficiency. Several methods of determining the spatial distribution of fuel during the engine cycle have been employed in the past. High speed photography works for the liquid phase of a spray, but is insensitive to the vapor phase. Early laser-induced fluorescence methods could not distinguish between liquid and vapor.

A new laser-induced fluorescence method for determining fuel distribution has been under development in the last decade. Exciplex-based liquid/vapor visualization systems allow two-dimensional fluorescent images of the liquid and vapor phases to be taken separately, using a diode array detector. Calibration of fluorescence intensity then permits the determination of concentration maps of liquid and vapor fuel. Developing such a quantitative calibration was the focus of this work.

1.1 Introduction to Exciplex

Melton (1) developed the concept of spectrally separated fluorescence emission from the liquid and vapor phases. His first application was to a spray from a hollow cone injector (2). Bardsley et al. (3,4) were the first to use the exciplex technique in an internal combustion engine. These earlier applications were strictly qualitative in nature.

More recent efforts have focused on developing quantitative calibrations for the exciplex method relating fluorescence intensity to mass concentration of fuel. Such a quantitative interpretation of the fluorescent images is possible because fluorescence intensity is directly proportional to the mass concentration of the fluorescing compound. Melton (5) developed calibration procedures based on the calculation of light absorption,

quantum yields, and other photophysical parameters. However, those procedures required that each parameter be correctly determined, and therefore the overall accuracy depended on the accuracy of a series of separate procedures. Rotunno et al. (6) developed direct calibration procedures for the liquid and vapor phases. These procedures involved direct measurement of the fluorescence intensity of a known amount of liquid or vapor. The direct procedures are simpler and believed to be more accurate by the developers, but they acknowledge that the photophysics-based procedures are more useful for experimental design of exciplexes. The calibration efforts stated above were for an exciplex system that is coevaporative with decane-based fuels, such as diesel fuel, whose normal boiling points are in the 200 to 300 degree Celsius range.

Current efforts are focusing on the development of exciplex systems that are coevaporative with automotive gasolines. Melton (7) is developing two systems that are expected to be coevaporative with fuels whose boiling points are in the 70 to 110 degree Celsius range. Shimizu et al. (8) developed a system meant for gasoline also. The normal boiling point of this system is 193 degrees Celsius, significantly higher than the boiling point of gasoline and therefore not an accurate marker. Use of such a system will result in underestimation of the true vapor concentration, since the fuel will evaporate more quickly than the fluorescent marker. However, Shimizu et al. took a unique approach in developing their calibration. Instead of presenting their vapor phase calibration as a spatial map of concentrations, they presented it in the form of a spatial map of equivalence ratios. They did not calibrate the liquid phase, but did use its fluorescence to show whether or not liquid fuel was present.

Murray and Melton (9) developed another use for exciplex laser-induced fluorescence. They devised a two-dimensional method for visually determining droplet temperatures in a fuel spray using exciplexes.

The focus of this project was to develop a quantitative calibration for an exciplex liquid/vapor visualization system. Since this was the first work with the exciplex method

at the Michigan State University Engine Research Laboratory, the naphthalene/N,N,N',N'-tetramethyl-p-phenylenediamine (TMPD) system was used, as this has been the most successful of those under development. The direct calibration procedures of Rotunno et al. (6) were adapted for this development work.

1.2 An Example of Fluorescent Images of a Fuel Distribution

To give an example of these fluorescent images and demonstrate how such a calibration is used, several images were taken in a research engine fitted with a quartz cylinder under motored conditions. The laser beam was focused into a horizontal sheet and passed through the quartz cylinder as shown in Figure 1. The images were taken

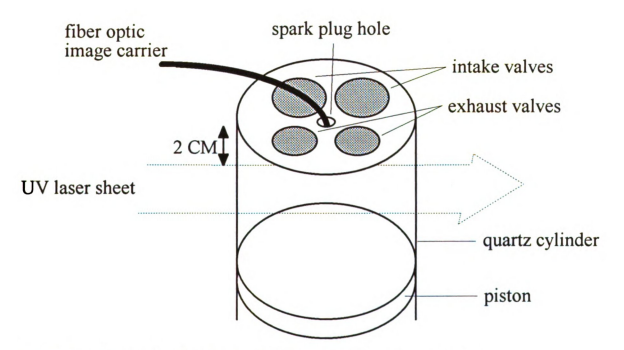


FIGURE 1: Schematic of engine in which fluorescent images were taken.

perpendicular to the light sheet through a fiber optic image carrier placed in the spark plug hole and are shown in Figure 2. These images are for an example only, they are not exciplex. The fluorescence is due to both liquid and vapor combined.



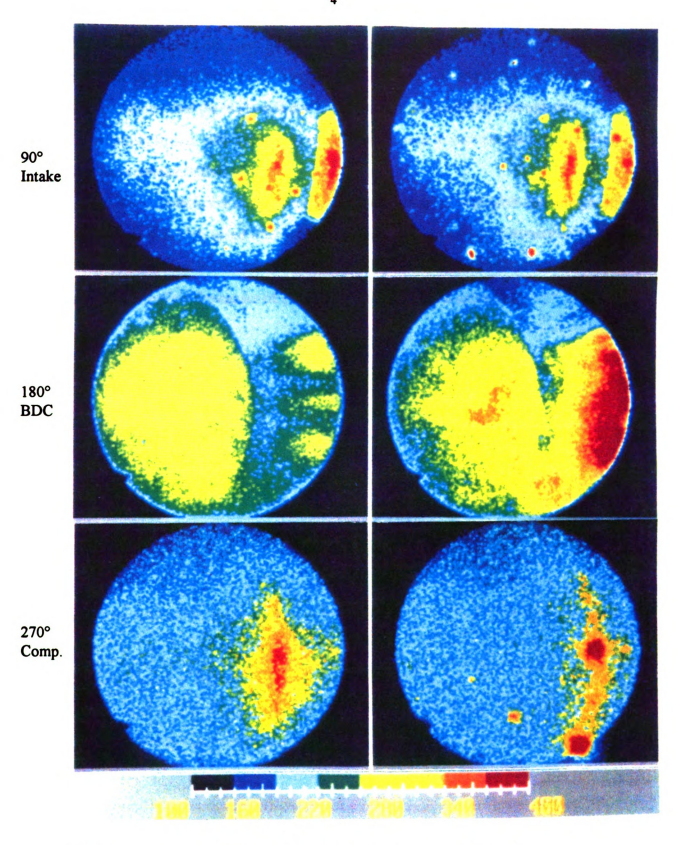


FIGURE 2: Fluorescent images of the fuel distribution in an engine cylinder.

The detector only sees light intensity, not wavelength. The colors were assigned by a look-up table based on the measured intensity level. The variation in intensity across the bore shows that the mixture is not homogeneous, even halfway through the compression stroke. The calibration would then be used to convert the intensity levels into mass concentrations of fuel.

The non-intrusive exciplex method could be coupled with other laser diagnostic methods such as high speed flow visualization and laser doppler velocimetry to provide information on fuel motion as well as fuel distribution. Such a combination of methods would help explain the causes of a resultant fuel distribution pattern.

CHAPTER 2

THE EXCIPLEX MECHANISM

2.1 System Composition

In order for an exciplex system to be an effective marker of the liquid and vapor phases, the components must be virtually coevaporative in the boiling range of the solvent. The naphthalene/TMPD system is coevaporative with decane based fuels, such as diesel fuel, whose normal boiling points are in the 200 to 300 degree Celsius range. A system consisting of 10% naphthalene, 1% TMPD, and 89% decane by weight was used for the development of this calibration.

Two additional exciplex systems have been developed by Melton (7) which are expected to be coevaporative with solvents boiling in the 70 to 110 degree Celsius range. These systems are expected to track the vaporization of automotive gasoline effectively. The first system consists of 10% triethylamine, 0.5% fluorobenzene and 89.5% hexane, and is expected to be coevaporative with a normal boiling point of 69 degrees. The second system consists of 10% n-propyldiethylamine, 0.5% 4-fluorotoluene and 89.5% isooctane, and is expected to be coevaporative with a normal boiling point of approximately 100 degrees.

2.2 Separation of Phases

The basic chemical mechanism is the same for all exciplex-based systems, but the specific chemical components are different. They all contain three basic components: a monomer, a ground state reactant, and a solvent which serves as the fuel. In the system used here, TMPD is the monomer (M), naphthalene is the ground state reactant (G), and decane is the solvent. The exciplex is formed in the reversible equilibrium

$$M^* + G \iff E^*$$
 (2-1)

where M* is the first excited singlet state of the monomer, and E* is the exciplex, which is short for excited state complex (6). The equilibrium of equation (2-1), which governs the formation of the exciplex in the liquid but not the vapor, is controlled by adjusting the concentration of the ground state reactant. The wavelength of the excitation source determines which excited electronic state is reached during the absorption transition (10). The monomer TMPD requires excitation at approximately 350 nm.

Figure 3 illustrates the individual steps of the exciplex mechanism. In the liquid

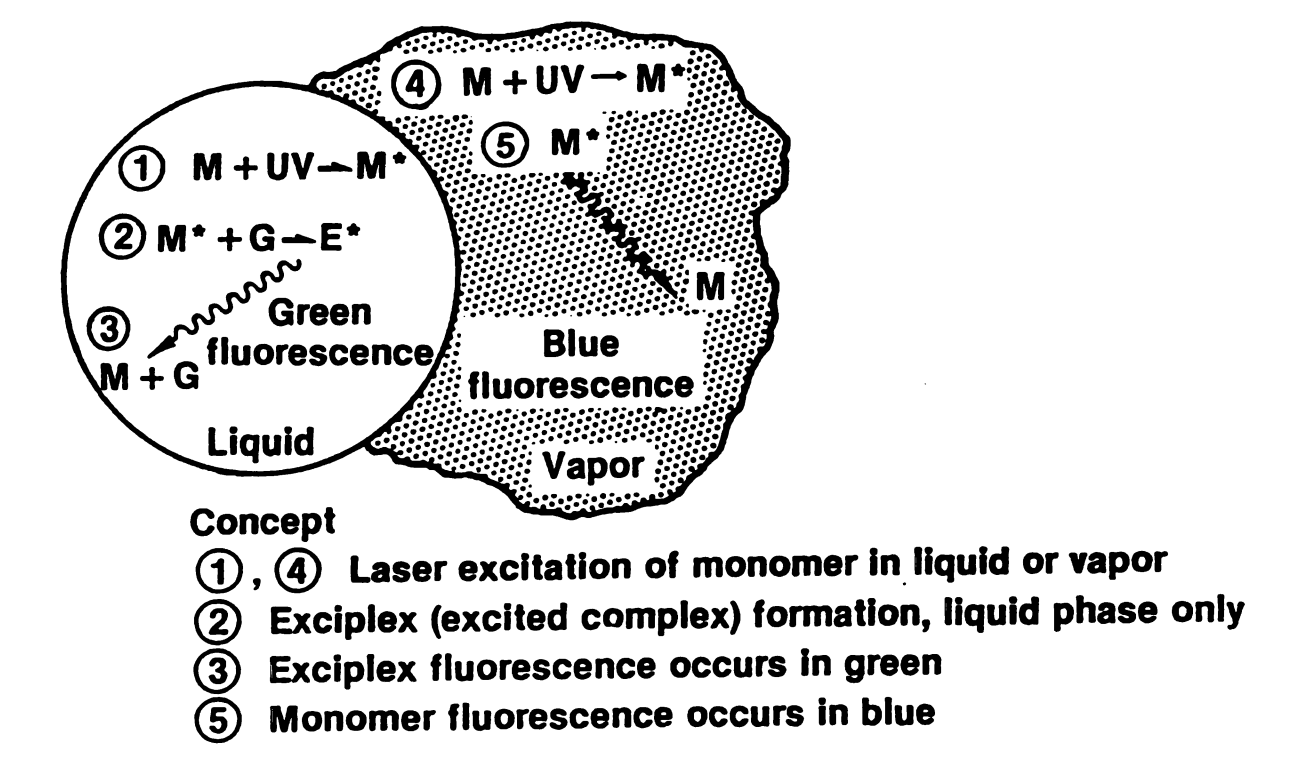


FIGURE 3: The mechanism of Exciplex liquid/vapor visualization systems.

phase, an excited TMPD molecule combines with a naphthalene molecule to form an exciplex. The exciplex then fluoresces as the molecules return to the ground state. In the vapor phase, the exciplex does not form. Instead, the excited TMPD molecule itself

fluoresces as it returns to the ground state. Since the formation of the exciplex results in it having a lower energy level than the excited monomer, its emission is also at lower energy. The energy of an emitted photon is given by

$$E = hc/\lambda \tag{2-2}$$

where h is Planck's constant, c is the speed of light, and λ is the wavelength. Therefore, the exciplex emission occurs at longer wavelengths than that of the monomer. Figure 4 shows the fluorescence emission spectra of the two phases. Using appropriate bandpass filters then allows fluorescent images of the liquid and vapor phases to be taken separately.

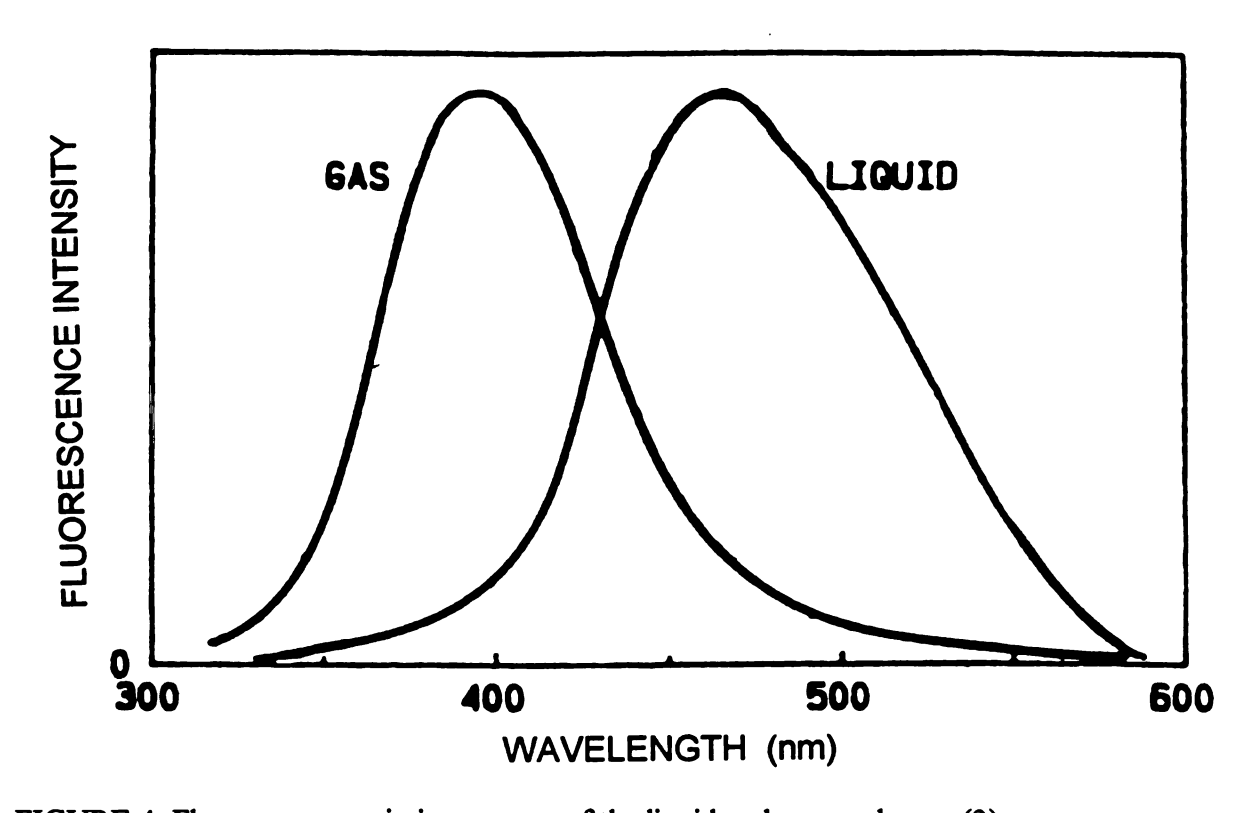


FIGURE 4: Fluorescence emission spectra of the liquid and vapor phases. (3)

CHAPTER 3

EXPERIMENTAL EQUIPMENT AND CALIBRATION PROCEDURE

3.1 Major Equipment

Descriptions of the experimental equipment and their features will be given separately to avoid interrupting the procedure with these details.

3.1.1 UV-Visible Absorption Spectrophotometer

To determine vapor concentrations, absorbance measurements were made with a Varian model Cary 1E UV-Visible absorption spectrophotometer. A spectrophotometer, which is generally used in analytical chemistry, can make absorbance measurements at a specific wavelength or produce a spectrum, i.e. absorbance over a range of wavelengths. This project only required measurements to be made at a single wavelength. The Cary 1E is a dual beam instrument. The collimated beam from the light source is chopped and directed alternately through the sample and a reference. Absorbance is then determined by comparison of the two beams' intensities with a photo multiplier tube. Adjustable slits in the monochromator section control the spectral bandwidth, while gratings control the wavelength. The spectrophotometer is controlled by a Dell 325D computer (with math coprocessor and GPIB board) through an IEEE488 interface using Varian drivers and software

3.1.2 Temperature-Controlled Sample Heating System

A temperature-controlled sample heating system was designed and constructed to vary the vapor concentration of a sample during the vapor phase calibration. A schematic of the system is shown in Figure 5.

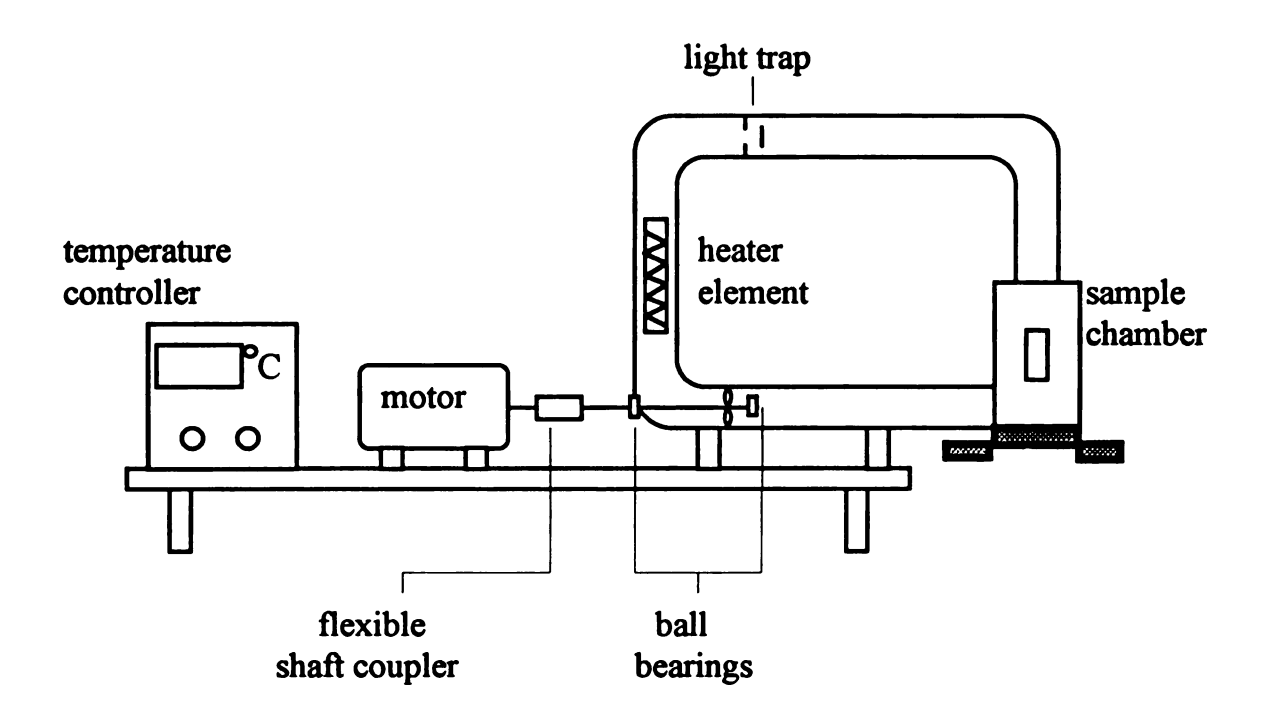


FIGURE 5: Schematic of temperature-controlled sample heating system.

Air is circulated through the sample chamber in a closed loop of 2.0 inch copper pipe. Since the system is capable of reaching temperatures of several hundred degrees Celsius, the fan is driven by an externally mounted motor. A 1/15 horsepower Dayton motor and variable speed control were used. A flexible shaft coupler was used to connect the motor to the fan blade shaft to prevent heat transfer from the fan blade shaft into the motor. The fan blade shaft is supported by ball bearings at two points. The standard bearing grease was removed and the bearings were repacked with Dow Corning 41 Extreme High Temperature Bearing Grease. The maximum operating temperature of the heating system is limited to 288 degrees Celsius (550 degrees F) by this silicone lubricant.

A Master Appliance 260 degree Celsius (500 degree F) heat gun element was used to heat the air, though higher temperature elements are available. The element was insulated thermally and electrically from the copper pipe with mica insulation. The inside

of the heating loop was painted flat black and light traps were constructed to prevent visible radiation from the heating element from reflecting into the sample chamber and causing error in the absorption or fluorescence intensity measurements. Air temperature is controlled with an Omega model 4001-KC proportional controller with K-type thermocouple input and relay output. The heating element is controlled by the relay output via an external contactor due to its power requirement. The controller input thermocouple is located in the air stream just above the sample holder. A second thermocouple is placed between the sample holder block and sample cuvet to measure the sample temperature. The mass of the holder and cuvet keeps the sample temperature nearly constant even though the air temperature fluctuates 8 to 10 degrees per controller cycle.

The sample chamber has optical access windows mounted on three sides for making absorption and fluorescence measurements. The windows are T20 Suprasil clear fused quartz discs from Heraeus Amersil. The sample holder is mounted in the sample chamber such that air can pass over all sides of the sample cuvet.

3.1.3 Excimer Laser and Laser Energy Meter

Ultraviolet excitation for the fluorescence was provided by a Lambda Physik model EMG160TMSC tunable excimer laser. This is a pulsed laser which can operate at wavelengths of 193, 248, 308, and 351 nm by changing the gas mixture and optics. Tuning mode produces a beam with a narrower bandwidth than power mode. This model contains two laser heads, an oscillator head and an amplifier head. In tuning mode, the oscillator and tuning optics produce a narrow bandwidth beam which is injected into the amplifier head for power amplification. The beam is also vertically polarized.

The laser was operated at 351 nm using a gas mixture of xenon, fluorine, and helium. At 351 nm, it produces an 18 nanosecond FWHM pulse with a rated maximum pulse energy of 70 mJ. In actual use, the pulse energy was initially higher but then

dropped below this value with age and use of a gas fill. According to a Lambda Physik service representative, a gas fill should be good for approximately 1,000,000 shots or 2 weeks.

A Scientech Vector series laser power/energy meter system was used to measure the pulse energy during the calibration. The system consists of the models S200 single channel power and energy indicator with digital readout, P25 25 mm pyroelectric detector, and VS25UV quartz beamsplitter with a 3.35/82.5 R/T ratio. The beamsplitter must be used because the detector's coating cannot handle the full 38 MW/sq. cm peak power density of the excimer laser. The beamsplitter reflects only 3.35 percent of the beam into the detector and transmits 82.5 percent. The R/T ratio can be entered into the indicator so that it will display the energy or power of the transmitted beam. The beamsplitter was calibrated with S polarized light and therefore must be positioned such that the reflected beam is directed vertically when used with the excimer laser. The indicator displays energy, average energy or power. It also collects and calculates statistics on a user-defined sample size of pulses.

3.1.4 Intensified CCD Detector

Fluorescent images were taken with a Princeton Instruments intensified CCD (Charge Coupled Device) detector system and stored on the Dell computer running Princeton Instruments CSMA (CCD Spectrometric Multichannel Analyzer) imaging and spectroscopy software. A model ICCD-576 G/RB detector was controlled by a model ST-130 controller. A model FG-100 pulse generator provided external high voltage gate pulses to the intensifier. The intensifier acts as the shutter and exposes the 576 x 384 pixel array when it receives a gate pulse. The time between array readouts is specified by the exposure time set in the software. The intensifier is controlled separately from readout, thereby permitting multiple array exposures per readout in External Sync timing

mode. This results in on-chip averaging which improves signal-to-noise over in-memory averaging.

The detector only sees light intensity, not wavelength. The images are assigned colors based on intensity values by a look-up table in the software when displayed on the monitor. Several look-up tables are included in the software, or the user can create customized tables. User defined look-up tables can be used to change the resolution of an image and to specify preferred shades of colors. The CSMA software also has image processing capabilities such as adding, subtracting or rotating images, and defining a rectangular region of interest on which to do statistics or zoom in.

3.1.5 Isolated Droplet Generator

Liquid droplets of a known size were required for the liquid phase calibration. An isolated droplet generator designed and constructed in the Department of Chemistry at Michigan State University was used for this purpose (11,12). The droplet generator is based on the principles of induced breakup of a liquid jet discovered by Rayleigh. Its electronic control module can be operated in a stand-alone mode or, for greater versatility, in a computer-controlled mode.

Figure 6 shows the basic components of the droplet formation module. Liquid is forced through a glass capillary to form a liquid jet. A rectangular piezoelectric crystal called a bimorph is attached to the capillary. When an oscillating voltage is applied to the bimorph, it deflects, causing the capillary to vibrate at the oscillation frequency. These vibrations are transmitted through the capillary to the surface of the liquid jet. Normally, the jet would travel in a cylindrical mass for some distance before it breaks up under the action of surface tension into a series of randomly sized drops. However, if the capillary is vibrated and the wavelength of the vibrations is greater than the circumference of the jet, the break up occurs in a uniform manner and produces droplets of uniform size and spacing.

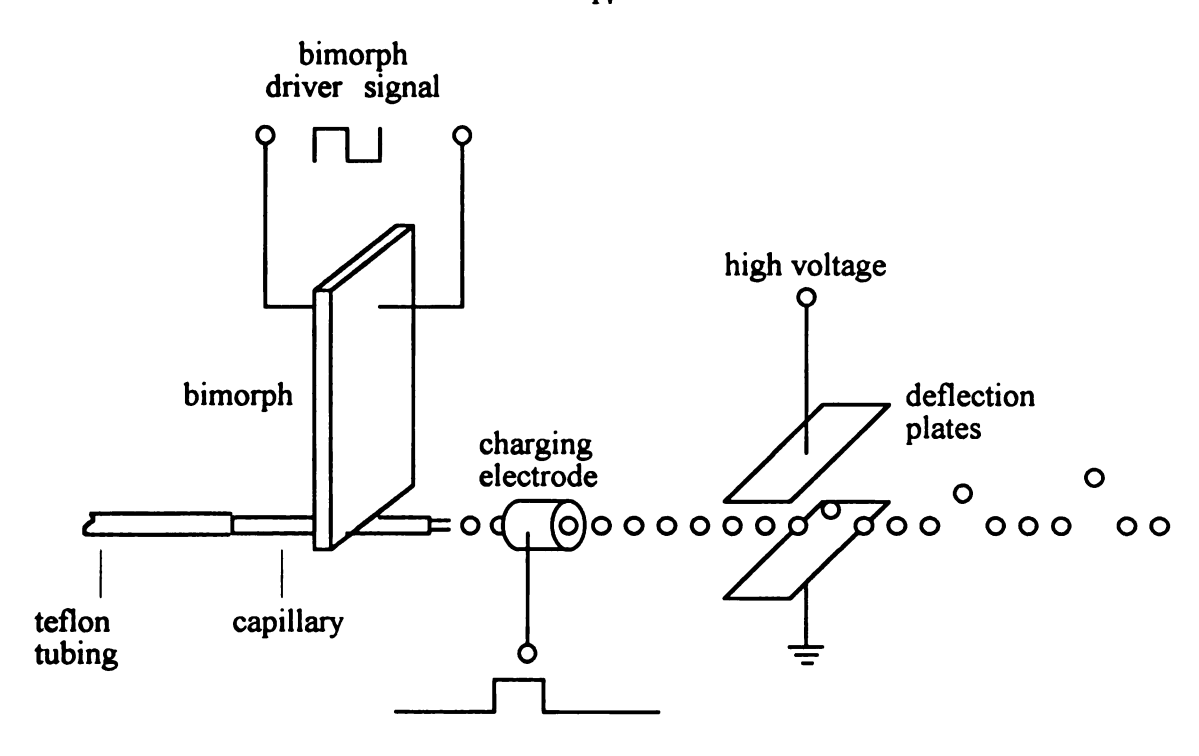


FIGURE 6: Schematic of the droplet formation module of the isolated droplet generator.

This droplet generator can theoretically produce droplets at rates of 1000 to 50,000 per second (13). Because the production rates are greater than desired for some experiments, this droplet generator has the ability to charge and deflect droplets out of the main stream so that they can be trapped. Selected droplets are charged as they pass through a cylindrical electrode as shown in Figure 6. They are then deflected as they pass between the high voltage plates and trapped, thereby decreasing the delivery rate in the main stream. The ratio of charged to uncharged droplets can be varied.

Droplet size and production rate are controlled by capillary size, bulk flow rate through the capillary, and applied bimorph frequency. Capillaries range in size from 10 to 65 microns inside diameter. Liquid is supplied by a constant pressure delivery vessel. Regulated pressure from a nitrogen gas cylinder is used to control the flow rate. Flow rate versus pressure has to be calibrated for each capillary. The liquid delivery system

contains a 2 micron in-line filter to keep the capillaries from getting clogged. Droplet volume can be calculated by

$$V_{d} = F/f \tag{3-1}$$

where F is the bulk flow rate and f is the production frequency. By substituting the formula for the volume of a sphere, droplet radius can be expressed as

$$r_d = (3F / 4\pi f)^{1/3}$$
 (3-2).

The overall error in the determination of the droplet radius by this method is reported to be on the order of 0.33 percent (11).

For this work, the isolated droplet generator was operated using 15 to 45 micron diameter capillaries, 20 to 60 psi liquid delivery pressures, and 7000 to 28,000 Hz applied bimorph frequencies. At production rates up to 28,000 Hz, droplet charging and deflection was not required as the droplets were visibly separated in the fluorescent images.

3.2 Procedure

The following explains the procedure used to calibrate an exciplex system. A separate calibration is required for each of the two phases.

3.2.1 Vapor Phase

The vapor phase calibration was carried out in two steps using a sample of TMPD, the vapor phase marker. The first step was to determine the vapor concentration versus temperature for the sample. The second step was to determine fluorescence intensity versus vapor concentration using the concentration/temperature relationship from the first step to establish known concentrations.

3.2.1.1 Sample Preparation

For the vapor phase calibration, a small sample of TMPD was prepared using a standard quartz fluorimeter cell with a stem and 10 mm light path length from NSG Precision Cells. Before placing the sample in the cuvet, an absorbance measurement was made on the empty cuvet with the spectrophotometer. This is the blank signal and was used to subtract the effect of the cuvet walls from the subsequent sample measurements.

TMPD was dissolved in spectrophotometric grade hexane to make a solution with a concentration of approximately 1.0 gram TMPD/liter. Approximately 100 microliters of solution was then transferred to the cuvet using a microliter syringe fitted with a 10 inch hypodermic needle so that the sample could be placed on the bottom of the cuvet, keeping the walls optically clear. The hexane was evaporated at room temperature. Because of the narrow opening in the cuvet stem, the hexane evaporated extremely slowly. The process was greatly speeded by attaching the hypodermic needle to a supply line and blowing dry nitrogen gas across the surface of the solution. The sample cuvet was then attached to a vacuum line, frozen with liquid nitrogen, evacuated, and sealed under vacuum.

Two samples were prepared. Sample 1 contained 100 microliters of solution and was evacuated to 10⁻³ torr. Sample 2 contained 125 microliters of solution and was evacuated to 10⁻⁴ torr. Sample preparation was done using the facilities of the Department of Chemistry.

3.2.1.2 Determination of Vapor Concentration Versus Temperature

The first step was to determine the vapor concentration versus temperature from absorbance measurements with the spectrophotometer. Increasing the temperature of the sample increases the vapor concentration by increasing the saturation vapor pressure. The temperature-controlled sample heating system was mounted in the sample compartment of the spectrophotometer for this purpose as shown in Figure 7. Measurements were made

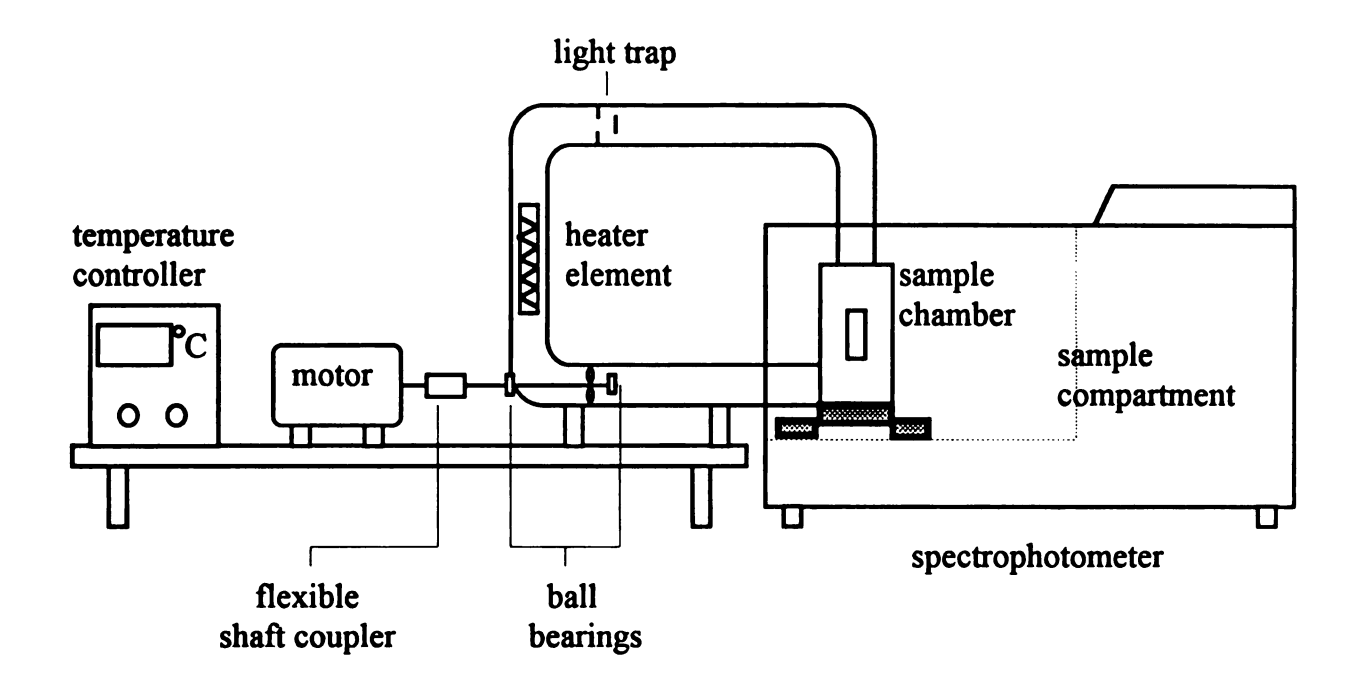


FIGURE 7: Schematic of setup for determining vapor concentration.

at 20 degree Celsius intervals from room temperature to 180 degrees.

The spectrophotometer was allowed to warm up approximately one-half hour and zeroed with the sample chamber windows of the heating system in the sample beam. This removes the effect of the windows from the measurements. The reference beam was empty, i.e. air was the reference. The sample was then placed in the sample chamber of the heater and absorbance measurements taken after the temperature equilibrated at each interval. The spectrophotometer settings used are in Table 1. After subtracting the blank signal, concentration was calculated using Beer's Law

$$A = \epsilon b c \tag{3-1}$$

where A is the absorbance, ε is the molar absorptivity (1.74 x 10⁴ L/mol· cm at 266 nm), b is the path length, and c is the unknown concentration.

TABLE 1: Spectrophotometer settings used for making absorbance measurements.

Parameter	Setting
photometric mode	absorbance
abscissa mode	sample number
wavelength	266 nm
spectral bandwidth	1.0 nm FWHM
source lamp	UV
sample averaging time	1.0 sec

3.2.1.3 Determination of Fluorescence Intensity Versus Vapor Concentration

The second step in the vapor phase calibration was to determine fluorescence intensity versus vapor concentration using the vacuum sealed TMPD sample. Again, temperature was used to vary the vapor concentration of TMPD, except that the concentration at each temperature was known from the first step. The setup for this step utilizes the sample heating system, excimer laser, laser energy meter, light sheet forming optics, and intensified CCD detector as shown in Figure 8.

The excimer laser was used as the excitation source, operating at a wavelength of 351 nm. The laser beam was passed through a custom-made variable beamsplitter with removable quartz discs for adjusting the pulse energy to the desired level, and a field stop to cut off the fringes. It then passed through the beamsplitter for the energy meter, a cylindrical focusing lens with a 300 mm focal length, a cylindrical recollimating lens with a -300 mm focal length to form a 550 nm wide vertical sheet, and the sample in the heating system.

Images of the fluorescence were taken perpendicular to the laser sheet at approximately 20 degree Celsius increments with the intensified CCD detector. The system was synchronized by externally triggering the CCD detector from the excimer laser. Several images were taken at each concentration level using 10 exposures per

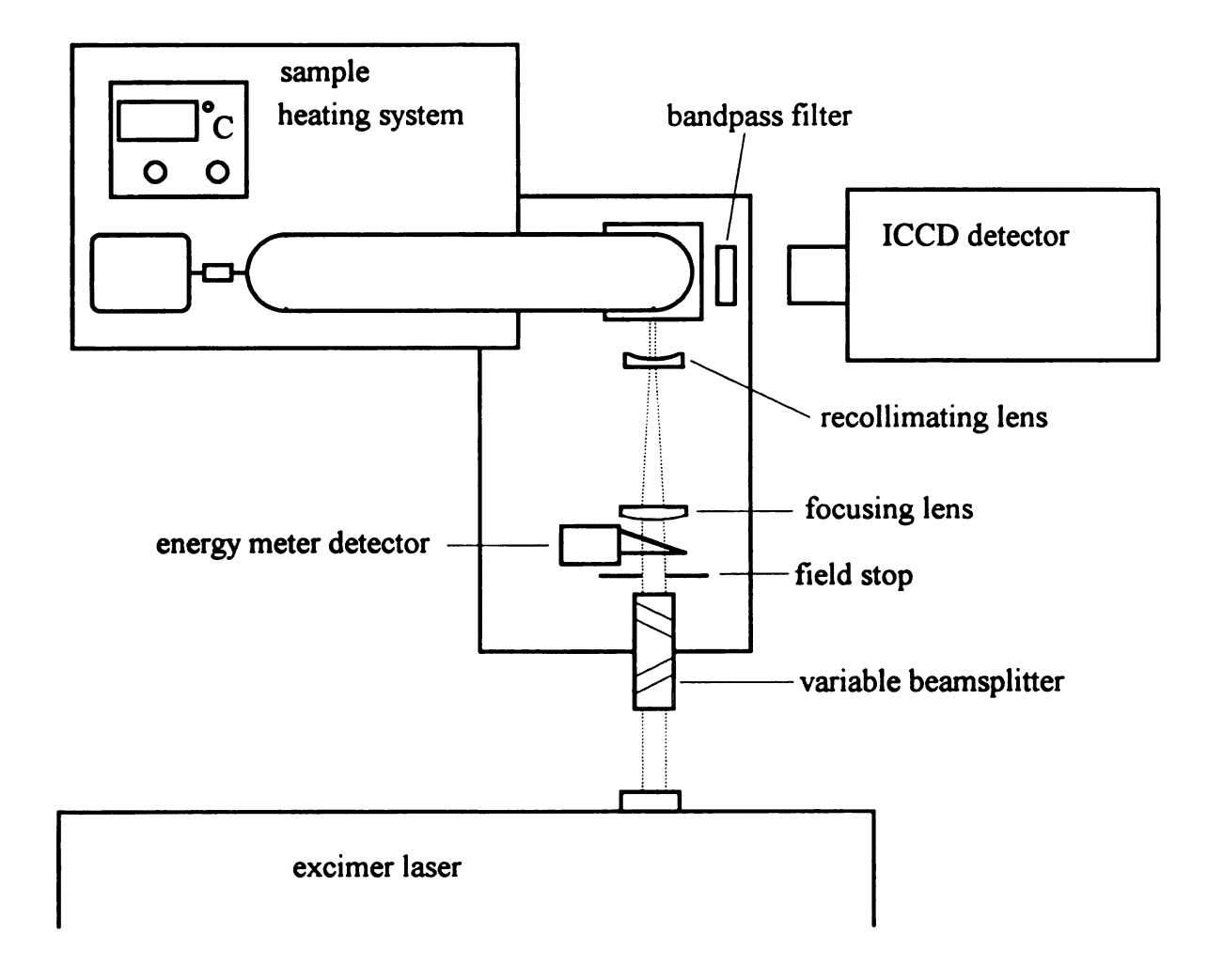


FIGURE 8: Schematic of setup for determining fluorescence intensity of vapor phase.

readout with background subtraction, and stored on the computer's hard disk. The average pulse energy of the 10 pulses most nearly associated with each image was recorded for image processing later. The system components and user-defined parameter values for this step of the calibration are given in Table 2. The detector hardware parameters are adjusted by ten-turn potentiometers but are not linear with the turn units on the dial face. Calibrations for these potentiometers along with other operational information to assist the user are contained in the Appendix.

TABLE 2: System components and parameter values for vapor phase calibration.

Component Laser	Parameter rep. rate charging voltage	<u>Value</u> 5 Hz 22 - 24 kV
Detector optics	extension tube zoom aperture apparent focal distance bandpass filter	18 mm 50 mm f/16 4.0 ft 400nm; 40nm FWHM
Detector hardware	gain delay gate pulse width	variable 640 250 ns
Detector software	timing mode exposure time image size background subtraction	ext. sync. normal 2.0 sec bin by 2 on

Fluorescence intensity data was extracted from the images using the CSMA software. A rectangular region of interest containing the cuvet image (except the edges) was defined, and the average intensity per pixel was calculated. The region of interest remained the same for all images. The average intensities were normalized by the pulse energy, corrected for detector gain, and corrected for the attenuation effects of the quartz windows and cuvet walls. Finally, the intensities were plotted resulting in a calibration curve of fluorescence intensity versus mass concentration of TMPD vapor. The concentration of fuel vapor is then inferred based on the mixture ratio of TMPD to fuel.

Figure 9 shows the temperature-controlled sample heating system mounted in the sample compartment of the spectrophotometer for the first step of the vapor phase calibration. Figure 10 shows the quartz windows in the sample chamber of the heating

system with the insulation removed. Figure 11 shows the heating system, CCD detector, and sheet forming optics setup for the second step of the vapor phase calibration.



FIGURE 9: Setup for determining vapor concentration.

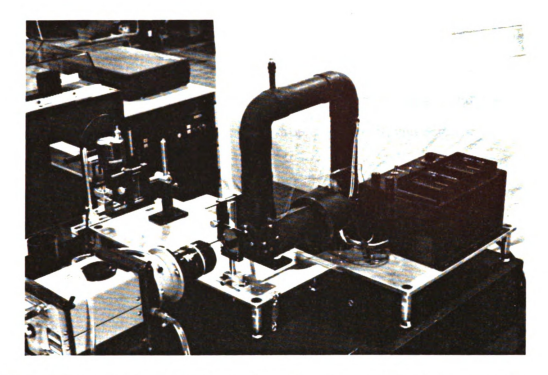


FIGURE 10: Temperature-controlled sample heating system with insulation removed.

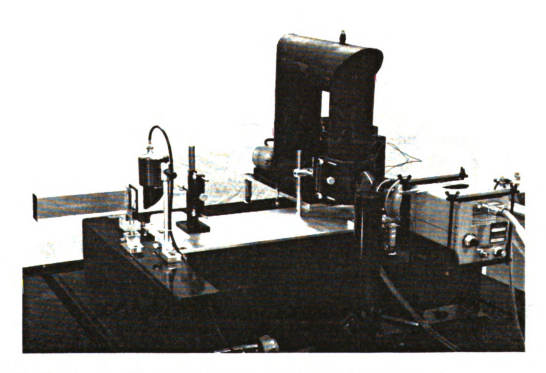


FIGURE 11: Setup for determining fluorescence intensity of vapor phase.

3.2.2 Liquid Phase

The liquid phase calibration was carried out in a single step by taking fluorescent images of known sized droplets of exciplex-doped fuel with the CCD detector. The total fluorescence intensity of the droplets was then calculated from the images and plotted versus droplet mass. A schematic of the laser, droplet generator, and detector configuration is shown in Figure 12.

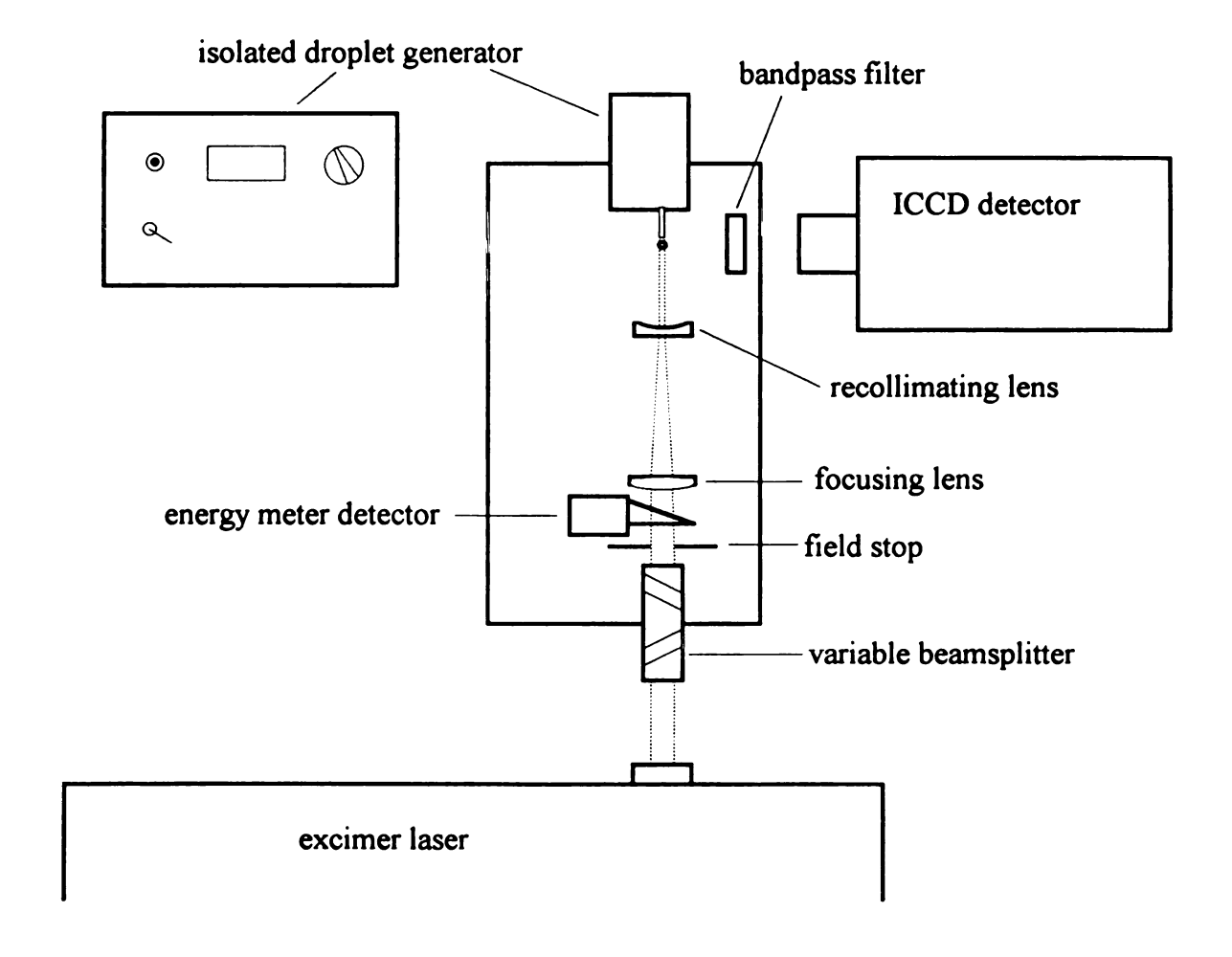


FIGURE 12: Schematic of setup for determining fluorescence intensity of liquid phase.

Again, the excimer laser provided excitation for the fluorescence and images were taken with the CCD detector. The sheet forming optics and energy meter configuration were the same as in the vapor phase, but the bandpass filter in front of the detector was now centered at 500 nm with a 40 nm FWHM bandwidth. The stream of droplets produced by the isolated droplet generator was directed downward through the vertical laser light sheet. Droplets were generated in the 75 to 200 micron diameter range by varying the flow rate through 20, 30 and 45 micron capillaries, and by varying the droplet production frequency from 7000 to 28,000 drops per second.

Fluorescence intensity data was extracted from the images by zooming in on individual droplets and calculating the total intensity by summing the intensity values of the pixels containing the droplet. Since this calibration could be done in the open atmosphere and no quartz windows or cuvets were in the optical path, the intensities only needed to be corrected for detector gain. The intensities were again normalized by the pulse energy and the result was a calibration curve of fluorescence intensity versus mass of liquid fuel.

The isolated droplet generator, sheet forming optics, and CCD detector setup for the liquid phase calibration are shown in Figure 13. Figure 14 is the droplet forming module showing the glass capillary and bimorph. Figure 15 is a fluorescent image of droplets taken during the liquid phase calibration at a droplet production rate of 28,000 per second. Figure 16 is a zoom of some droplets from Figure 15 using the image processing software. Each square is a pixel in the detector's array.

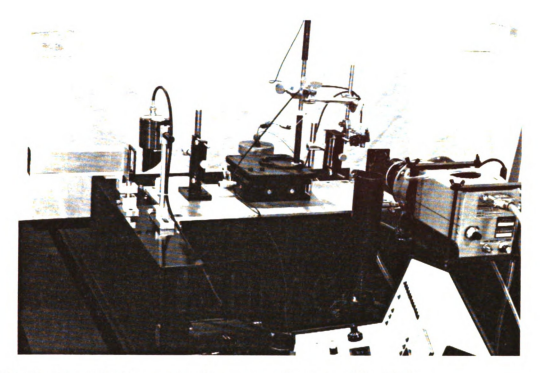


FIGURE 13: Setup for determining fluorescence intensity of liquid phase.

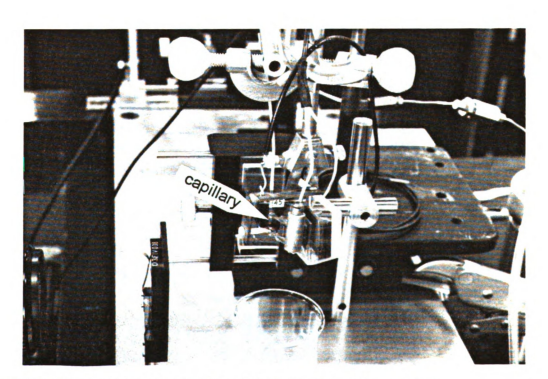


FIGURE 14: Droplet formation module of the isolated droplet generator.

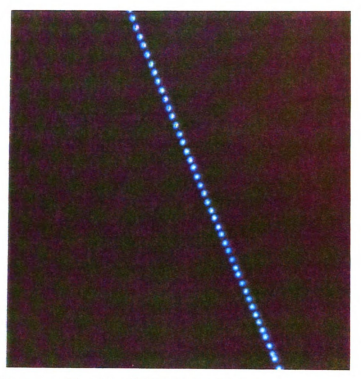


FIGURE 15: Fluorescent image of isolated droplets.

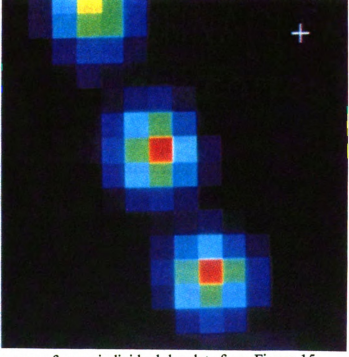


FIGURE 16: A zoom of some individual droplets from Figure 15.

CHAPTER 4

RESULTS AND DISCUSSION

4.1 Vapor Phase

The TMPD vapor concentration versus temperature for the first step of the vapor phase calibration is shown in Figure 17. The upper plateau is the result of the entire sample being vaporized. The absorbance measurements were corrected for the effect of the cuvet walls using the blank signal before being converted to concentration. As shown by the four runs, the measurements were quite repeatable.

Sample 1 was used primarily for testing and adjustment of the equipment, while the data being presented here were taken with sample 2. The maximum concentration of 12.26 micrograms/cc from Figure 17 times the volume of the cuvet results in a total sample size of 84.6 micrograms. The amount of TMPD placed in the cuvet during sample preparation was approximately 125 micrograms (125 microliters of 1.0 gram TMPD/liter solution). The difference is believed to be due to sublimation of TMPD during evacuation of the cuvet. Therefore, it is important that the sample only be evacuated long enough to remove the air from the cuvet.

After the TMPD sample has been heated and driven into the vapor phase, it recrystalizes on the surface of the cuvet upon cooling. It is desired that it do this on the bottom and not the walls where it would interfere with optical access. Therefore, the bottom of the cuvet should be cooled first. This feature happened to be inherent in the design of the heating system. The bracket from the external walls of the sample chamber attaches to the bottom of the cuvet holder. Thus, when the temperature is reduced, heat is conducted to the external walls from the bottom of the cuvet first.

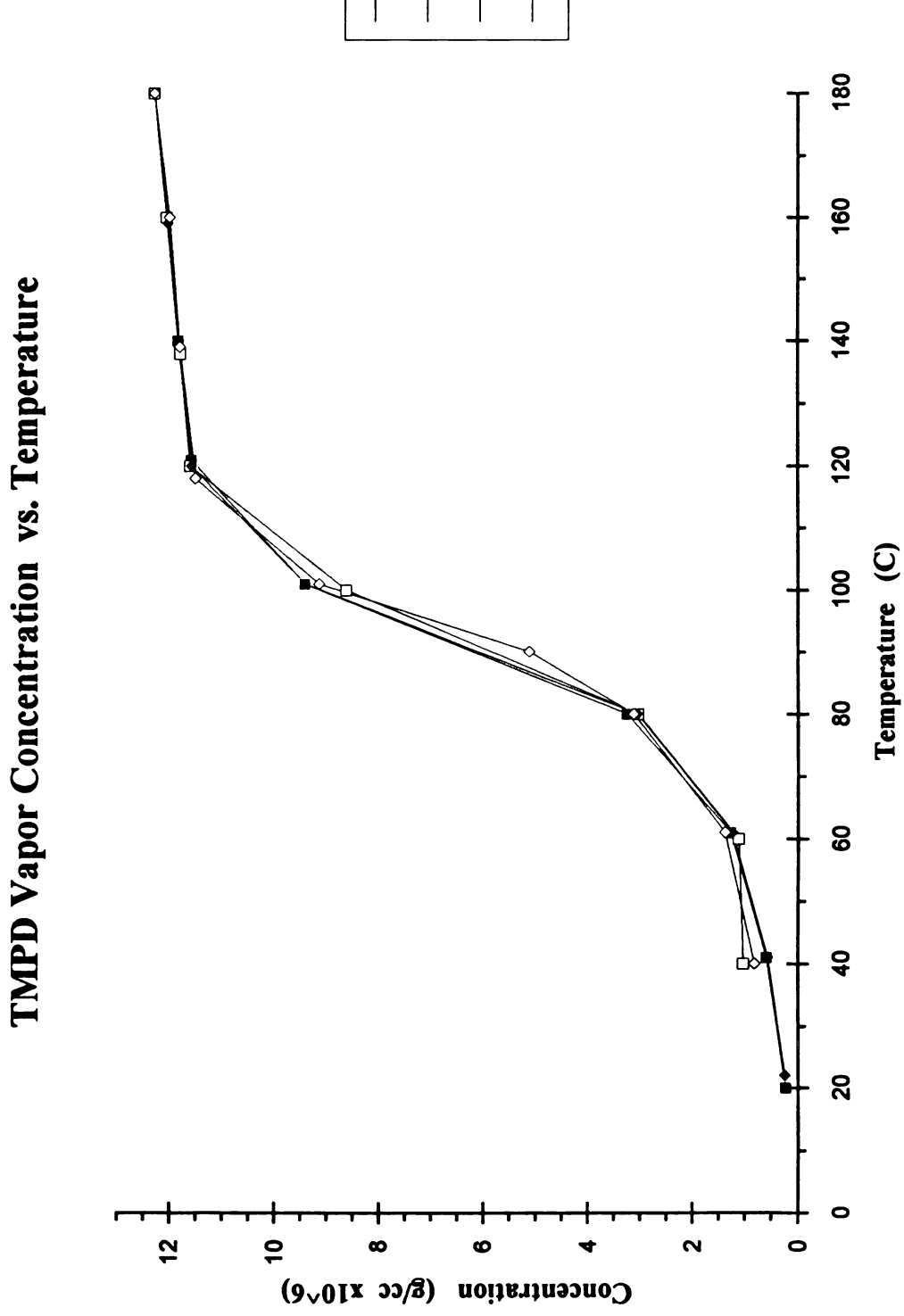


FIGURE 17: TMPD vapor concentration versus temperature for first step of vapor phase calibration.

The normalized fluorescence intensity versus vapor concentration data, as shown in Figure 18, is nearly linear, as expected, since fluorescence intensity is directly proportional to concentration. The calibration constant resulting from a linear regression curve fit is 8.19 counts/(microgram/cm³). The scatter at the higher concentrations may be due to temperature effects and should be investigated further. The fluorescence intensities were corrected for detector gain and for the attenuation of the window and cuvet wall using the transmittance of these components. The transmittances were measured with the spectrophotometer at 380 nm, the peak of the vapor phase emission. The transmittances of the window and cuvet wall were also measured at 351 nm and used to correct for attenuation of the incident laser pulse energy.

The fluorescence intensities were normalized by the incident laser pulse energy. Incident laser pulse energy determines how many molecules are put in the excited state, and the number of excited molecules determines fluorescence intensity. In other words, fluorescence intensity is proportional to pulse energy as well as concentration, but normalized fluorescence intensity is proportional to concentration.

The excimer laser emits a 5 mm wide by 20 mm high rectangular beam with a 2 mm diameter dead spot in the center. The dead spot is caused by a spot of reflective coating in the center of the laser's output coupler. When the beam was focused in the horizontal direction to form a vertical sheet, the intensity profile was not uniform. This could be seen as a dark band passing horizontally through the center of a fluorescent image taken perpendicular to the sheet. Since this would affect the fluorescence intensity measurements, only the portion of the image above the dark band was used for extracting data. Other ways of dealing with the dead spot would be to use only the portion of the beam between the spot and side of the beam or between the spot and top of the beam, and use optics to form the desired size sheet.

Melton et al. observed the development of a brown discoloration on the inside of the cuvet walls where the laser enters and exits after continual irradiation. In this work,

Normalized Fluorescence Intensity vs. TMPD Vapor Concentration □ \□ . . . 12 9 Concentration (g/cc x10^6) 120 T 0 5 20 8 8 6 Normalized Fluorescence Intensity

Regr.

FIGURE 18: Normalized fluorescence intensity versus TMPD vapor concentration.

the walls of sample 1 gradually became clouded around the entrance and exit points of the laser, but sample 2 did not. Also, the TMPD in sample 1 turned brown, but that in sample 2 did not. The difference is believed to be due to the degree of evacuation. Sample 1 was evacuated to 10^{-3} torr, while sample 2 was evacuated to 10^{-4} torr. Therefore, more complete removal of air from the cuvet is important to reducing the photoreaction caused by the laser.

Oxygen is an efficient quencher of TMPD fluorescence, but nitrogen is not (6). As a result, fuel distribution studies in engines must be done with nitrogen under motored conditions. Exciplex systems that are not quenched by oxygen need to be developed so that studies can also be done in a firing engine.

4.2 Liquid Phase

A plot of the normalized fluorescence intensity versus droplet mass for exciplex-doped decane is shown in Figure 19. The fluorescence intensities were again corrected for the detector gain and normalized by the incident laser pulse energy.

Droplet sizes were not predetermined because not all frequency and flow rate combinations of the droplet generator could produce stable droplets. As a result, droplet sizes were completely random, but there were more than enough combinations that could produce stable droplets. An attempt was made to produce smaller droplets using a 10 micron capillary. This capillary would produce a stable liquid jet with straight decane, but the jet would exit in random directions with exciplex-doped decane. Apparently, dissolving naphthalene in the decane made it too viscous.

The data in Figure 19 showed more scatter than expected. The scatter is believed to be due to hot spots in the laser beam. The intensity profile of the beam was not measured and quantified, but a profile of the beam using thermal paper showed dark spots scattered throughout. (The darker the paper, the greater the intensity.)

The calibration of fluorescence intensity versus droplet mass shown in Figure 19 is

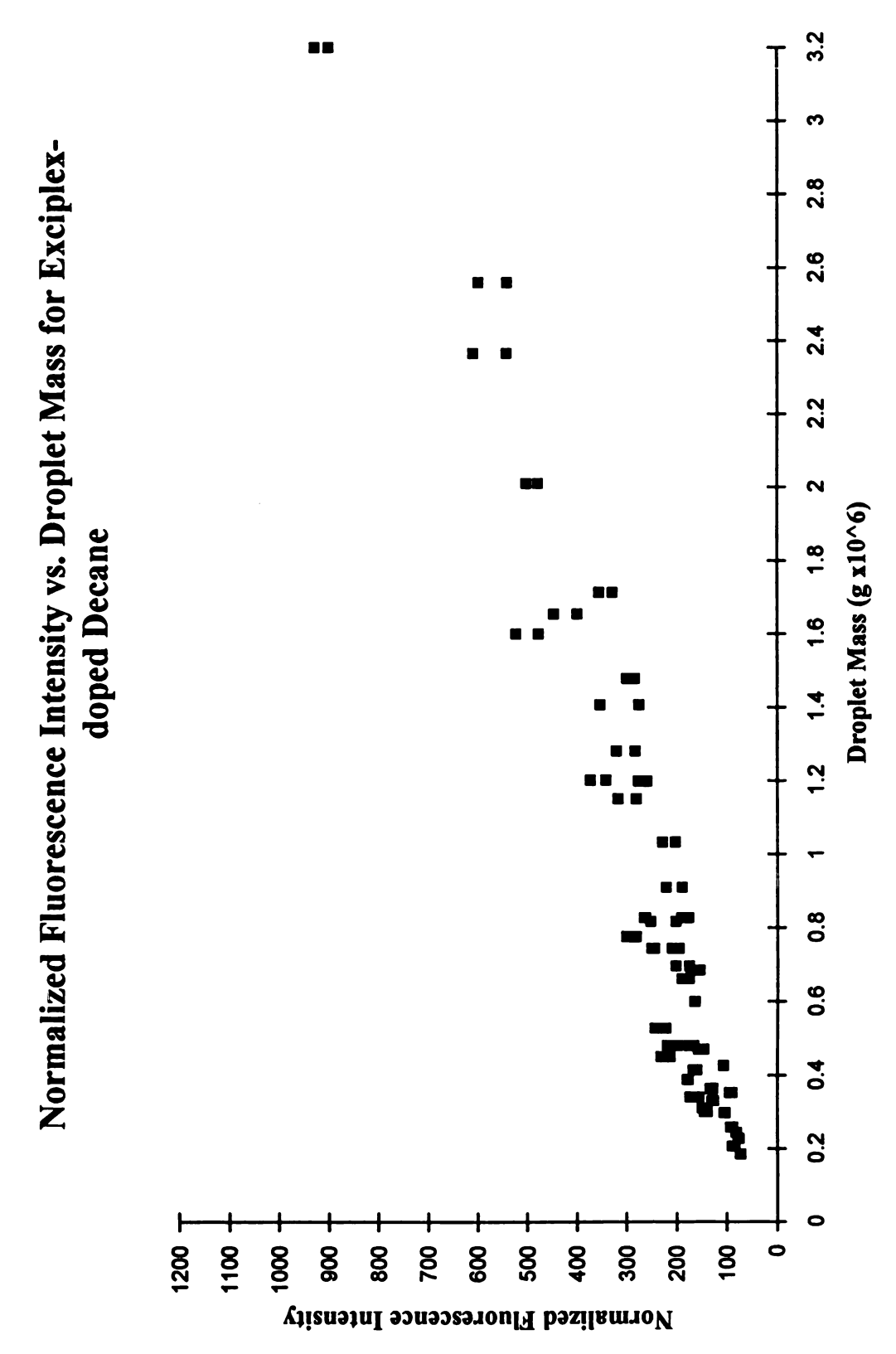


FIGURE 19: Normalized fluorescence intensity versus droplet mass.

not linear. This nonlinearity is due to the larger droplets being optically thick, i.e. having optical densities greater than 0.2 (6). An optical density of 0.2 corresponds to a droplet diameter of approximately 80 microns (13). In an optically thick droplet, the laser intensity decreases as it passes through the droplets, causing the total fluorescence intensity to be decreased.

For optically thin droplets, those with optical densities up to 0.2, the calibration curve should be linear. So, instead of using single droplets that were not optically thin at the larger masses, a new method was developed. This method adds up the masses and fluorescence intensities of several small droplets, which are individually optically thin, to generate the calibration at the larger masses. The result was a linear calibration curve of fluorescence intensity versus mass of liquid fuel as shown in Figure 20. The calibration constant from a linear regression curve fit is 398.81 counts/microgram. Since the droplets from a high pressure diesel (a decane based fuel) injector are primarily in the optically thin regime, a calibration developed with optically thin droplets would be desired.

Normalized Fluorescence Intensity vs. Liquid Mass using Multiple **Droplet Summation**

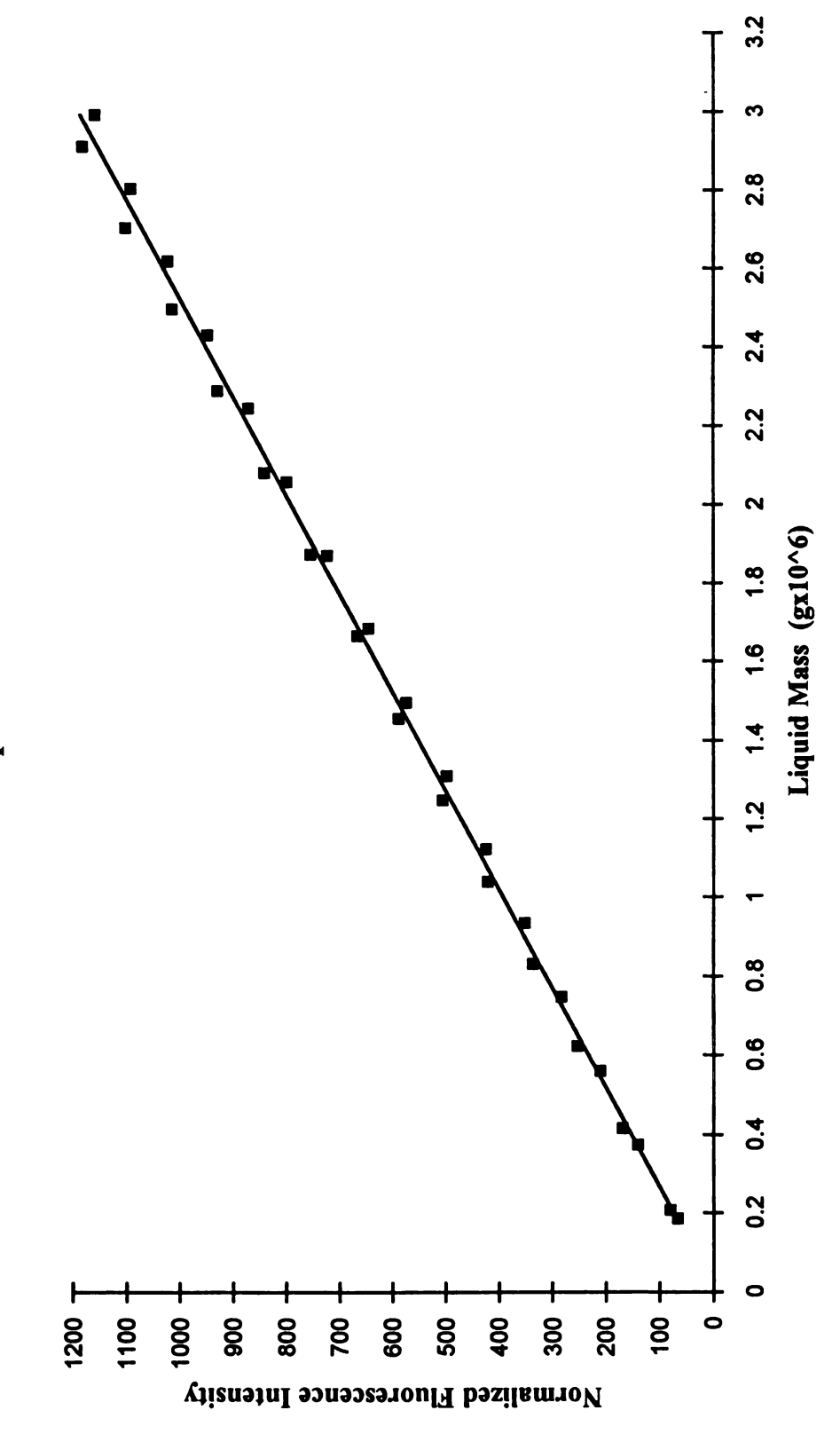


FIGURE 20: Normalized fluorescence intensity versus liquid mass using multiple droplet summation.

CHAPTER 5

SUMMARY AND CONCLUSIONS

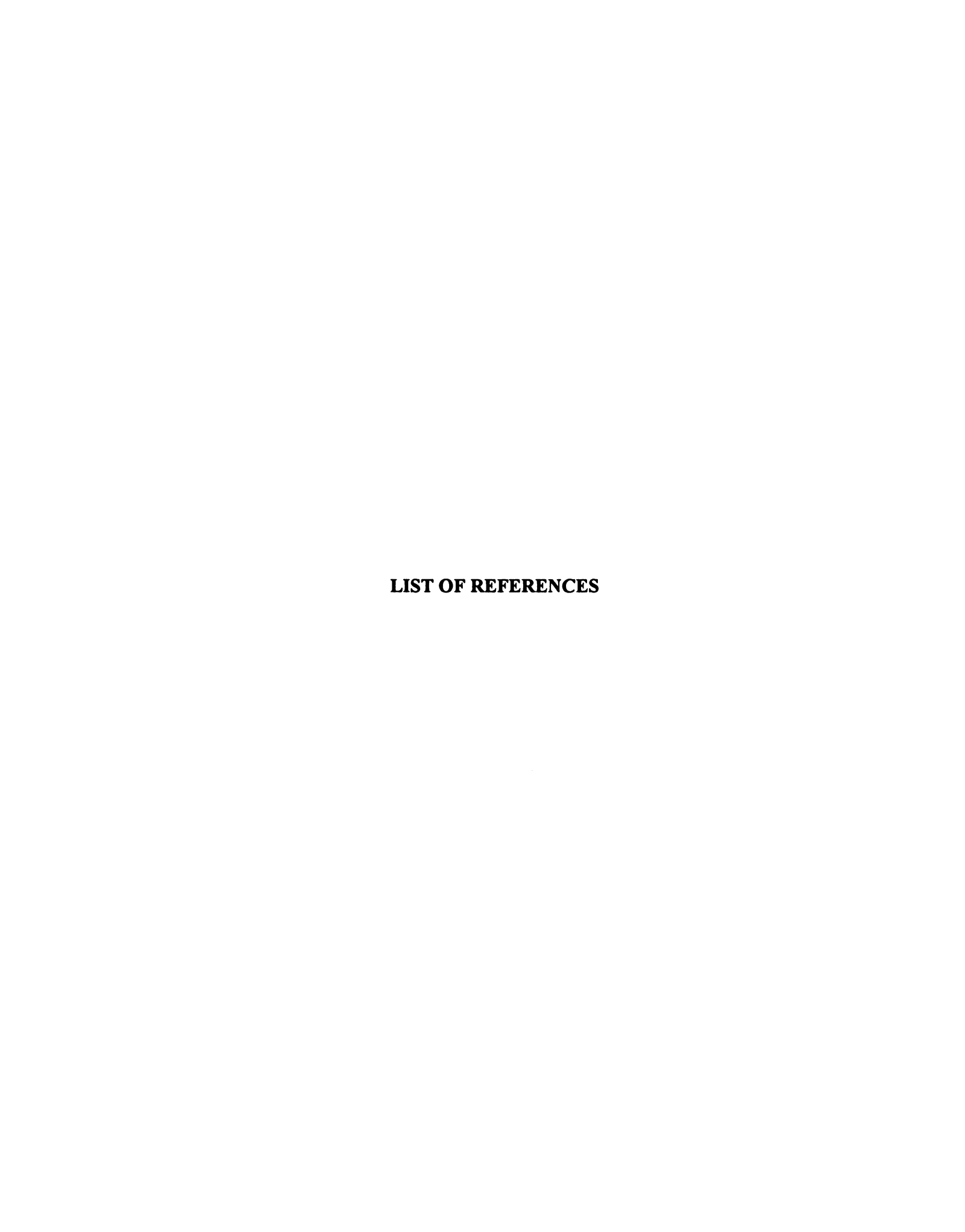
- 1. Exciplex liquid/vapor visualization would be a useful tool for quantitatively studying fuel distribution in internal combustion engines and combustors.
- 2. Multiple droplet summation of optically thin droplets should be used to generate liquid phase calibration curves for use in studies with high pressure injectors.
- 3. The effects of optical access windows in a setup can be removed by measuring their transmittance at the appropriate wavelength. This allows a single calibration to be used for setups with different elements in the optical path.
- 4. Since a calibration is setup-dependent, preliminary fluorescent images should be taken in the setup before calibrating to determine the required ranges of the calibrations.
- 5. The cuvet should be cooled from the bottom after taking data so that the TMPD recrystallizes on the bottom and doesn't interfere with optical access by recrystallizing on the walls.
- 6. Fluorescence intensity is proportional to pulse energy and should be normalized.
- 7. The dead spot in the center of the excimer laser's beam must be dealt with when focusing the beam into a sheet.
- 8. Significantly less clouding and discoloration of the cuvet walls was observed in a sample evacuated to 10⁻⁴ torr when compared to one evacuated to 10⁻³ torr. Also, the sample should be evacuated only long enough to remove the air, in order to prevent significant loss of TMPD. Therefore, a high vacuum line should be used to evacuate the sample for a short period of time.

- 9. The vapor phase fluorescence from the naphthalene/TMPD system is strongly quenched by oxygen. Fuel distribution studies in engines using this system can only be done with nitrogen under motored conditions.
- 10. The isolated droplet generator produced uniformly sized and spaced droplets of known size and was very well suited for this application.

CHAPTER 6

RECOMMENDATIONS

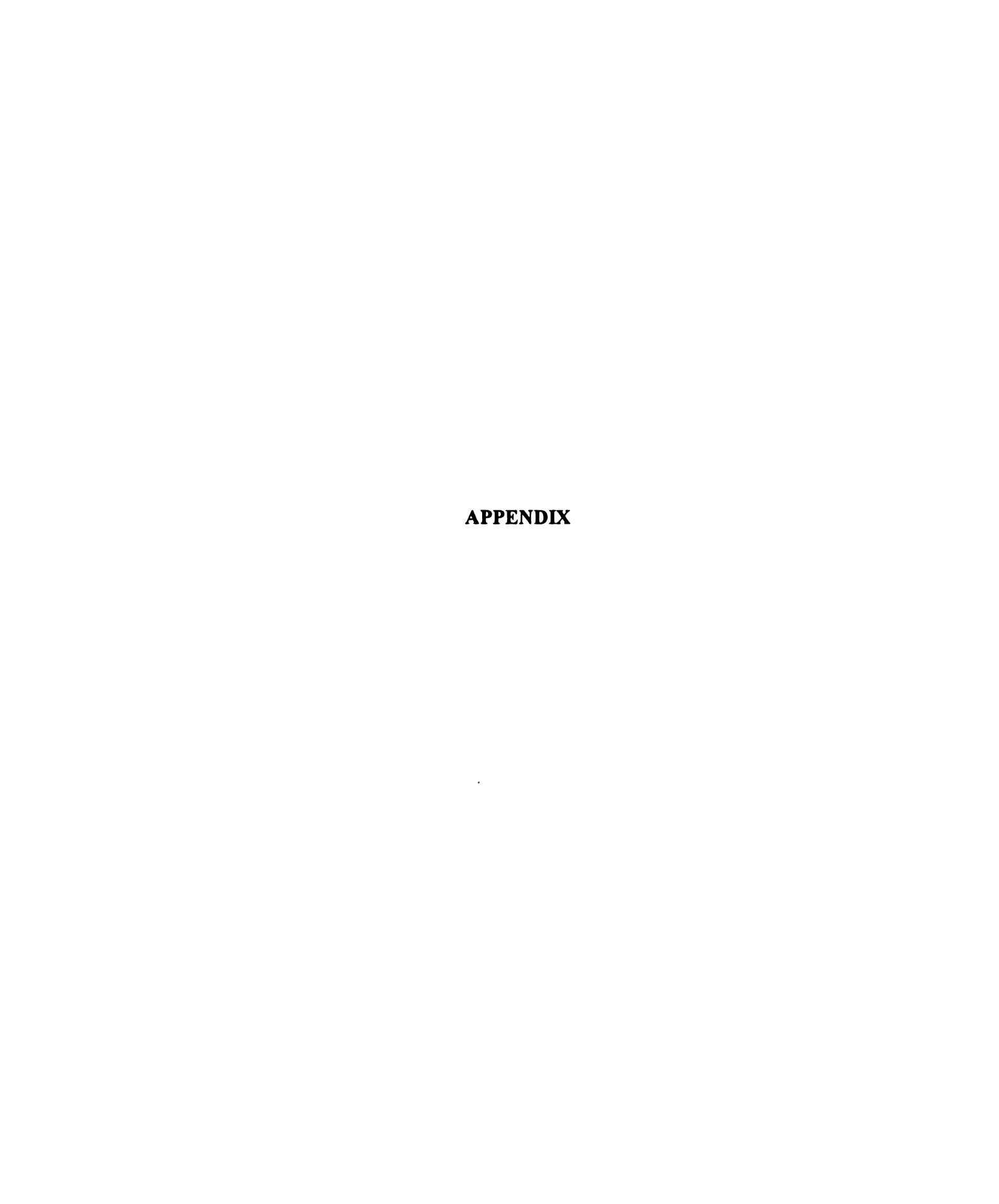
- 1. The effects of high temperatures on fluorescence intensity should be investigated.
- 2. The development of exciplex systems for other fuels needs to be continued.
- 3. Exciplex systems which will work in an oxygen environment need to be developed.
- 4. Methods should be investigated for making the laser beam intensity profile more uniform.
- 5. The use of fiber optic image carriers for exciplex imaging should be studied.
- 6. The percent of TMPD evaporated versus the percent of fuel evaporated from a droplet, at the temperature at which fuel distribution studies will be done, should be investigated to determine how accurately the TMPD tracks the vapor.



LIST OF REFERENCES

- 1. Melton, L. A., "Spectrally Separated Fluorescence Emissions for Diesel Fuel Droplets and Vapor", Applied Optics, Vol. 22, No. 14, pp. 2224-2226, 1983.
- 2. Melton, L. A. and Verdieck, J. F., "Vapor/Liquid Visualization in Fuel Sprays", Twentieth Symposium (International) on Combustion, (The Combustion Institute, 1984), pp. 1283-1290.
- 3. Bardsley, M. E. A., Felton, P. G. and Bracco, F. V., "2-D Visualization of Liquid and Vapor Fuel in an I. C. Engine", SAE Paper 880521, 1988.
- 4. Bardsley, M. E. A., Felton, P. G. and Bracco, F. V., "2-D Visualization of a Hollow-Cone Spray in a Cup-in-Head, Ported, I. C. Engine", SAE Paper 890315, 1989.
- 5. Melton, L. A., "Quantitative Use of Exciplex-Based Vapor/Liquid Visualization Systems (A Users Manual)", Final Report, Army Research Office Contract DAAL03-86-K-0082, 1988, (NTIS order # ADA191649).
- 6. Rotunno, A. A., Winter, M., Dobbs, G. M. and Melton, L. A., "Direct Calibration Procedures for Exciplex-Based Vapor/Liquid Visualization of Fuel Sprays", Combust. Sci. and Tech., Vol. 71, pp. 247-261, 1990.
- 7. Melton, L. A., "Exciplex-Based Vapor/Liquid Visualization Systems Appropriate for Automotive Gasolines", Applied Spectroscopy, Vol. 47, No. 6, pp. 782-786, 1993.
- 8. Shimizu, R., Matumoto, S., Furuno, S., Murayama, M. and Kojima, S., "Measurement of Air-Fuel Mixture Distribution on a Gasoline Engine Using LIEF Technique", SAE Paper 922356, 1992.
- 9. Murray, A. M. and Melton, L. A., "Fluorescence Methods for Determination of Temperature in Fuel Sprays", Applied Optics, Vol. 24, No. 17, pp. 2783-2787, 1985.
- 10. Ingle, J. D. and Crouch, S. R., *Spectrochemical Analysis*, Prentice-Hall, Englewood Cliffs, New Jersey, 1988.

- 11. Weigand, P. M. and Crouch, S. R., "Evaluation of a Programmable, Hardware-Driven Isolated Droplet Generator", Applied Spectroscopy, Vol. 42, No. 4, pp. 567-571, 1988.
- 12. Wiegand, P. M., Ph.D. Dissertation, Michigan State University, East Lansing, 1985.
- 13. Archontaki, H. A. and Crouch, S. R., "Evaluation of an Isolated Droplet Sample Introduction System for Laser-Induced Breakdown Spectroscopy", Applied Spectroscopy, Vol. 42, No. 5, pp. 741-746, 1988.
- 14. Felton, P. G., Bracco, F. V. and Bardsley, M. E. A., "On the Quantitative Application of Exciplex Fluorescence to Engine Sprays", SAE Paper 930870, 1993.



APPENDIX

The Appendix contains information to assist the user in the operation of the equipment in this setup and is meant as a supplement to the equipment manuals.

A.1 Equipment Connections for Laser Induced Fluorescence Imaging

The connections for the ICCD detector system and excimer laser for the laser induced fluorescence portion of the project are shown in Figure 21. The connections

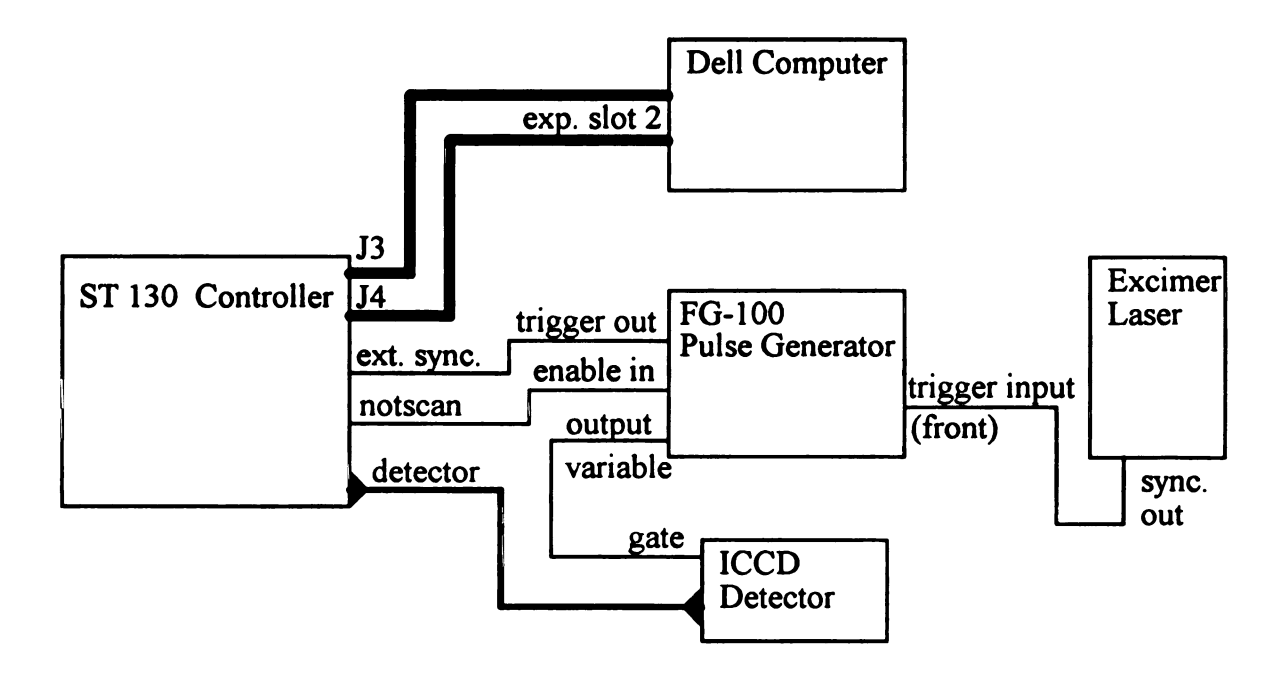


FIGURE 21: Connections for laser induced fluorescence equipment.

shown in Figure 21 are a combination of Case 1 and Case 2 in section 6.3.1, ICCD Gating Experiments Examples, of the Princeton Instruments manual. The timing diagram for this configuration is shown in Figure 22. The excimer laser triggers the pulse

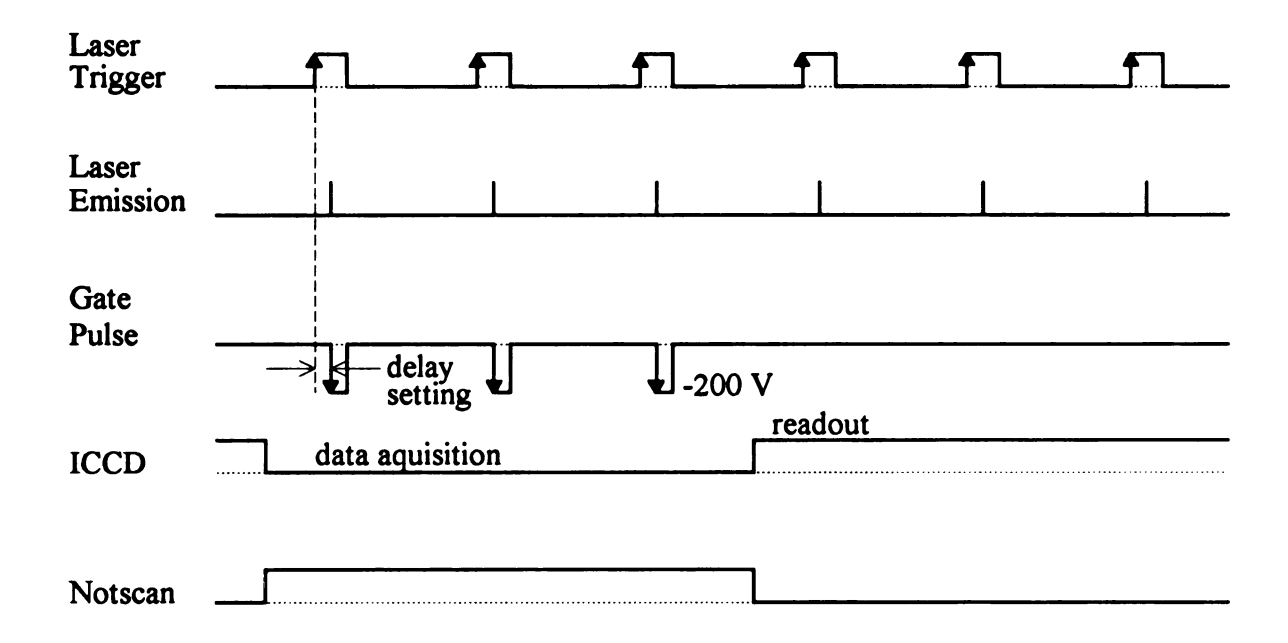


FIGURE 22: Timing diagram for ICCD detector system configuration.

generator which sends a high voltage gate pulse to the intensifier in the ICCD detector. The delay between the laser trigger and gate pulse is adjustable so that the detector can be gated after the laser emission occurs. The 'enable in' to 'not scan' connection prevents the array from being exposed during readout by blocking the gate pulses. The 'trigger out' to 'ext. sync.' connection initiates readout when the system is being externally triggered and the controller is being operated in the external synchronization mode. The time during which data is acquired is determined by the 'exposure time' set in the software. The number of exposures accumulated by the detector array per readout is determined by the exposure time and the laser repetition rate. For one exposure per readout, the exposure time can be set to zero or the laser repetition rate can be adjusted accordingly.

A.2 Operational Information for the Laser Induced Fluorescence Imaging System

The gain of the ICCD detector and the pulse width of the gate pulse generator are controlled by ten-turn potentiometers, but are not linear with the potentiometer setting. Experiments were done to determine the gain and pulse width versus potentiometer settings.

The ICCD detector gain is variable from 1 to 100 times. Table 3 summarizes the average intensity gain versus potentiometer setting for the detector. Potentiometer settings are read from 0 to 1000.

TABLE 3: Average intensity gain versus potentiometer setting.

Potentiometer setting	Intensity gain
1000	100.0
990	85.3
980	73.7
960	54.6
940	39.8
920	29.0
900	20.8
850	9.01
800	3.86
750	1.91
700	1.26
650	1.07

The pulse width of the FG-100 pulse generator is variable from 18 to 650 ns in range 1 of the variable width mode. A Tektronix 11302 oscilloscope was used to measure the pulse width. Table 4 summarizes the pulse width versus potentiometer setting.

TABLE 4: Gate pulse width versus potentiometer setting.

Potentiometer setting	Pulse width (ns)
1000	600 to 650
998	550
997	500
996	450
995	400
993	350
990	300
986	250
980	200
970	150
945	100
0	18

The potentiometer collar with the setting indicator mark on it must be turned clockwise when setting the position. There is a small amount of play in the collar which will affect the pulse width by as much as 50 ns. If the potentiometer is turned gently to 1000, the pulse width will be 600 ns. If light torque is applied to the knob, the pulse width will increase to 650 ns. All other positions were repeatable.

Another experiment was conducted to determine the gate pulse delay setting required to initiate detector gating immediately after the laser emission pulse, yet avoid gating before laser emission had decayed. This was necessary to ensure that the image intensities in the calibration were due only to fluorescence emission and not direct laser emission. It was carried out by focusing the detector on a piece of aluminum which scattered the laser pulse while emitting negligible fluorescence that would obscure the decay of the laser emission pulse. The laser pulse width is approximately 18 ns. The shortest detector gate pulse width, also of approximately 18 ns, was used. The maximum intensity of the images was then monitored while varying the delay setting. The peak image intensities occurred at a delay potentiometer setting of 624. Increasing or

decreasing the delay from 624 resulted in a decrease in the intensities. Therefore, the laser emission pulse and the detector gate pulse were completely overlapped at 624.

The absolute delay time could not be measured. However, the change in delay time for a given change in potentiometer setting could be measured with the oscilloscope. From this it was determined that the delay time increases 1.6 ns per unit change of the potentiometer setting.

Delaying the gate pulse an additional 20 ns should place the leading edge of the gate pulse 2 ns after the trailing edge of the laser emission pulse. This translated into a delay setting of 637. At this setting, the image intensities indicated that the trailing edge of some of the laser pulses was being caught by the gate pulse. This was probably due to trigger jitter in the excimer laser. A delay setting of 640 cleared this up and was used for the calibration.

Changing the gate pulse width does not affect the delay setting required. The trailing edge of the gate pulse moves when the pulse width is changed. The leading edge remains fixed relative to the trigger.

